Published in final edited form as:
Comp Biochem Physiol C Toxicol Pharmacol. 2012 May ; 155(4): 573–579. doi:10.1016/j.cbpc.2012.01.007.

Glutathione transferase pi class 2 (GSTp2) protects against the cardiac deformities caused by exposure to PAHs but not PCB-126 in zebrafish embryos

Lindsey VT. Garner and **Richard T. Di Giulio**
Nicholas School of the Environment, Duke University, Box 90328, Durham, North Carolina, USA 27708

Abstract

Glutathione transferases (GSTs) are phase II enzymes that detoxify a wide range of toxicants and reactive intermediates. One such class of toxicants is the ubiquitous polycyclic aromatic hydrocarbons (PAHs). Certain PAHs are known to cause developmental cardiac toxicity in fish. Herein, we explored the role of GST pi class 2 (GSTp2) in PAH- and PCB-induced cardiac toxicity in zebrafish (Danio rerio) embryos. We measured expression of GSTp2 in embryos exposed to individual and co-exposures of the PAHs benzo[k]fluoranthene (BkF), benzo[a]pyrene (BaP), and fluoranthene (FL) as well as 3,3′,4,4′,5-pentachlorobiphenyl (PCB-126). GSTp2 mRNA expression was induced by exposure to BkF, BaP, PCB-126, and BaP + FL and BkF + FL co-exposure. A splice junction morpholino was then used to knockdown GSTp2 in developing zebrafish. GSTp2 knockdown exacerbated the toxicity caused by co-exposures to BkF + FL and BaP + FL. However, GSTp2 knockdown did not affect PCB-126 toxicity. These results further suggest that pi class GSTs serve a protective function against the synergistic toxicity caused by PAHs in developing zebrafish

Keywords

glutathione transferase; morpholino; polycyclic aromatic hydrocarbons; polychlorinated biphenyls; zebrafish; cardiotoxicity

1. Introduction

Polycyclic aromatic hydrocarbons (PAHs) are ubiquitous environmental contaminants that are often found in aquatic systems as mixtures. Many PAHs are agonists for the aryl hydrocarbon receptor (AHR), a ligand-activated cytosolic transcription factor. Upon ligand binding, the AHR translocates to the nucleus, dimerizes with the aryl hydrocarbon receptor nuclear translocator (ARNT), and binds to xenobiotic response elements (XREs) on genes encoding various phase I and II enzymes that in turn metabolize PAHs (Schmidt and Bradfield, 1996). The cytochrome P450s (CYPs), particularly CYP1A, are well-characterized phase I enzymes, and phase II enzymes known to be activated by the AHR include UDP-glucuronosyltransferases (UDPGTs), NAD(P)H:quinone oxidoreductase 1

Correspondence: Lindsay Van Tiem Garner, Phone 919-613-8059, lav3@duke.edu.

(NQO1), and glutathione transferases (GSTs; EC 2.5.1.18) (Denison et al., 2002; Nebert et al., 2000).

GSTs are a family of phase II enzymes that detoxify a wide range of toxicants and reactive intermediates. GSTs function by conjugating electrophilic substrates, both endogenous and exogenous, to reduced glutathione. The conjugates are generally less toxic than the unconjugated metabolite, more water soluble, and thus, more easily excreted from the cell. Certain GSTs also exhibit glutathione peroxidase activities by catalyzing the reduction of organic hydroperoxides into alcohols, and certain GSTs are induced in response to prooxidants in a variety of organisms (reviewed in Hayes et al., (2005). Seven classes of cytosolic GST enzymes (alpha, mu, pi, sigma, theta, omega, and zeta) have been identified in mammals and are grouped according to substrate specificity, amino acid sequence, and immunological crossreactivity; collectively they may comprise 2–4% of total cytosolic proteins in the liver (Hayes et al., 2005; Schlenk et al., 2008). While relatively little is known about GSTs in fishes, four classes (pi, mu, theta, and alpha) have been identified in salmonids (Donham et al., 2005); zeta, omega and the mitochondrial kappa GST have been identified in river pufferfish (*Takifugu obscures*) (Kim et al., 2010); and a unique piscine GST, initially characterized in plaice (*Pleuronectes platessa*) (Leaver et al., 1997), has been designated rho. Isoforms of alpha, mu, omega, pi, rho, theta, and a microsomal GST have been identified in zebrafish (*Danio rerio*) (Schlenk et al., 2008). The various GST isoforms have been shown to metabolize many environmental pollutants, including pesticides, antibiotics, and PAHs. Among the GST isoforms, the pi class has been shown to be highly efficient in conjugating carcinogenic benzo[a]pyrene (BaP) metabolites to glutathione (Robertson et al., 1986). In addition, it has been shown in mouse liver that the contribution of mGSTp1-1 in detoxifying the carcinogenic metabolite of BaP, (+)-anti-7,8-dihydroxy-9,10-oxy-7,8,9,10-tetrahydrobenzo[a]pyrene, is greater than the contribution of the other GSTs combined (Hu et al., 1997).

PAHs, as well as co-planar polychlorinated biphenyls (PCBs) and dioxins, cause a wide range of toxicities, and fish early life stages are particularly sensitive to the developmental toxicity caused by PAHs. Exposure to 2–4-ringed PAHs has been shown to alter heart morphology, impair heart looping, and cause atrioventricular conduction block in zebrafish (Incardona et al., 2004). Co-exposure to a PAH that is an AHR ligand (such as BaP, benzo[k]fluoranthene (BkF), or the model PAH β-naphthoflavone (BNF)) and one that is a CYP inhibitor (such as fluoranthene (FL) or the model PAH β-naphthoflavone (ANF)) causes severe pericardial effusion and the stringy heart phenotype in Atlantic killifish embryos (*Fundulus heteroclitus*) (Wassenberg and Di Giulio, 2004) and zebrafish embryos (Billiard et al., 2006; Van Tiem and Di Giulio, 2011). Our laboratory has previously shown that upregulated glutathione transferase pi class 2 (GSTp2) expression precedes the cardiac deformities caused by co-exposure of an AHR ligand and a CYP1 inhibitor in zebrafish (Timme-Laragy et al., 2009; Van Tiem and Di Giulio, 2011).

In this study, we sought to determine the role of zebrafish GSTp2 in mediating the cardiac toxicity caused by PAH co-exposures. We utilized morpholino gene knockdown to determine whether GSTp2 knockdown exacerbates or ameliorates the cardiac effects of the AHR agonists BkF and BaP individually and also in combination with the CYP1 inhibitor FL in zebrafish embryos. Additionally, we sought to compare the role of GSTp2 in PAH toxicity with its role in mediating the cardiac toxicity caused by exposure to 3,3′,4,4′,5-pentachlorobiphenyl (PCB-126), a non-*ortho*-substituted co-planar PCB that is the strongest PCB ligand for the AHR (Tillitt et al., 2008). Based on what is known regarding the metabolism of PAHs and PCB-126, we hypothesized that GSTp2 knockdown would increase the cardiac toxicity caused by PAH co-exposures but would not have an effect on PCB-126-induced cardiac toxicity.

2. Material and methods

2.1 Fish care

Adult EkkWill zebrafish (*D. rerio*; EkkWill Waterlife Resources, Ruskin, FL, USA) were maintained in a recirculating AHAB system (Aquatic Habitats, Apopka, FL, USA) at 28 °C under a 14:10 light:dark cycle. Adult fish were fed brine shrimp and a mix of Cyclop-eeze (Argent Chemical Laboratories, WA, USA) and Zeigler's Adult Zebrafish Complete Diet (Aquatic Habitats).

Embryos were collected after natural spawning of adult zebrafish and were maintained in 30% Danieau (Nasevicius and Ekker, 2000) in an incubator under the same conditions as adults. Adult care and reproductive techniques were non-invasive and approved by the Duke University Institutional Animal Care & Use Committee (A279-08-10).

2.2 Chemicals

Benzo[k]fluoranthene (BkF), benzo[a]pyrene (BaP), and fluoranthene (FL) were purchased from Absolute Standards, Inc. (Hamden, CT, USA), and 3,3′,4,4′,5-pentachlorobiphenyl (PCB-126) was purchased from AccuStandard (New Haven, CT, USA). Dimethyl sulfoxide (DMSO) and tricaine methanesulfonate (MS-222) were purchased from Sigma-Aldrich (St. Louis, MO, USA). BkF, BaP, FL, and PCB-126 stocks were dissolved in DMSO, protected from light, and kept at −20 °C.

2.3 Morpholino injection

Morpholino antisense oligonucleotides were designed and produced by Gene Tools, LLC (Philomath, OR, USA). A splice-junction morpholino targeting the exon 2-intron 2 boundary was designed to knockdown GSTp2 (GSTp2-mo; 5′-ATTTTCATACAAACCTTTGATAGCG-3′). Splice-junction morpholinos cause aberrant splicing of pre-mRNA, most commonly via deletion of the targeted exon or insertion of the targeted intron, and knockdown via splice-junction morpholino can be quantified using PCR. Gene Tools' standard control morpholino (Co-mo; 5′-CCTCTTACCTCAGTTACAATTTATA-3′) was used as a morpholino injection control. Both morpholinos were fluorescein-tagged at the 3′ end to monitor injection success. Morpholinos were diluted to either 100 mM or 250 mM working stocks in 30% Danieau.

Morpholinos (approximately 3 nL injection volume) were injected by hand into the yolk of zebrafish embryos at the 1–4 cell stage using a microinjection system consisting of a Nikon SMZ-1500 zoom stereomicroscope (Nikon Instruments Inc., Lewisville, TX, USA) and an MDI PM 1000 Cell Microinjector (MicroData Instrument Inc., S. Plainfield, NJ, USA). Embryos exhibiting normal development and strong, uniform incorporation of the morpholinos assessed via fluorescence microscopy were used for experiments.

2.4 Dosing

2.4.1 Dosing for deformities—At 24 hpf, embryos were dosed in 7.5 mL 30% Danieau in 20-mL glass scintillation vials (VWR, West Chester, PA, USA) with five embryos per vial and three vials per treatment. Using DMSO as a control, the four dosing regimes were as follows: 100 mg/L BaP, 500 mg/L FL, and 100 mg/L BaP + 500 mg/L FL co-exposure; 100 mg/L BkF, 100 mg/L FL, and 100 mg/L BkF + 100 mg/L FL co-exposure; 10 mg/L BkF, 200 mg/L FL, and 10 mg/L BkF + 200 mg/L FL co-exposure; and 1 mg/L PCB-126 and 2 mg/L PCB-126. The doses were chosen based on preliminary dose-response curves and so that the exacerbation or protection elicited by the GSTp2-mo could be measured compared to various levels of pericardial effusion severity in NI embryos. Final DMSO

concentrations were ≤ 0.03% across all treatments. Dosed embryos were maintained in an incubator at 28 °C until the time of deformity assessment.

2.4.2 Dosing for reverse transcription PCR and QPCR—For QPCR, non-injected (NI) embryos were dosed at 24 hpf in 7.5 mL 30% Danieau in 20-mL glass scintillation vials with five embryos per vial and six vials per treatment. DMSO was once again used as a control, and embryos were dosed with the three following regimes: 10 mg/L BkF, 200 mg/L FL, and 10 mg/L BkF + 200 mg/L FL; 100 mg/L BaP, 500 mg/L FL, and 100 mg/L BaP + 500 mg/L FL; and 1 mg/L PCB-126. For reverse transcription PCR, NI and GSTp2-mo (100 mM) embryos were dosed at the same time and manner with either DMSO or a co-exposure of 10 mg/L BkF + 200 mg/L FL. For QPCR and RT-PCR, embryos were dechorionated at 48 hpf, pooled in groups of ten (two vials), and fixed in RNA*later* (Applied Biosystems, Foster City, CA, USA). Samples were stored at −80 °C until RNA extraction.

2.5 Confirmation of GSTp2 splice-mo efficacy by reverse transcription PCR analysis

Samples were thawed on ice, homogenized with a sterile hand-held homogenizer in RNA-Bee for 30 s, and RNA was extracted according to the RNA-Bee protocol (Tel-Test Inc., Friendswood, TX, USA).

RNA quantity and quality were analyzed spectrophotometrically using a NanoDrop ND-100 (NanoDrop Technologies, Wilmington, DE, USA). cDNA was synthesized using the Omniscript Reverse Transcriptase kit (Qiagen, Inc., Valencia, CA, USA) according to the manufacturer's instructions with 500 ng RNA, random hexamers, and RNaseOut (Invitrogen, Carlsbad, CA, USA). The reaction was carried out in a Biometra T1 thermocycler (Göttingen, Germany) for 1 h at 37 °C.

RT-PCR was performed in a 25-mL reaction containing 62.5 ng template, 12.5 mL AmpliTaq Gold Master Mix (Applied Biosystems), 0.5 mL each 10 mM forward and reverse primer, and 9 mL distilled H_2O. Thermocycler conditions were as follows: 95 °C for 5 min; 35 cycles of 95 °C for 15 s, 58 °C for 15 s, and 72 °C for 4 min; and finally, 72 °C for 10 min. All reactions were performed in triplicate. To examine potential deletion of exon 2 or insertion of intron 2 by the GSTp2 splice-mo, the forward primer was located in exon 1 (5′-CAGCAACTTCACAGACCTCGCTTT-3′), and the reverse primer was located in exon 3 (5′-ATGTCACCCTTCATCCAGTCCT-3′). Primers were designed using PrimerQuest software (Integrated DNA Technologies, Inc., www.idtdna.com). Gel electrophoresis of 10 mL of PCR product was performed using 2% agarose gels stained with SYBR Safe DNA gel stain (Invitrogen). Gels were imaged with an AlphaImager HP (Cell Biosciences, Santa Clara, CA, USA).

2.6 QPCR

RNA extractions and cDNA synthesis were performed as described in Section 2.4. b-actin was used as a housekeeping gene, and b-actin and GSTp2 primers were published previously (b-actin, F: 5′-AAGATCAAGATCATTGCTCC-3′ and R: 5′-CCAGACTCATCGTACTCCT-3′ and GSTp2, F: 5′-TCTGGACTCTTTCCCGTCTCTCAA-3′ and R: 5′-ATTCACTGTTTGCCGTTGCCGT-3′) (Grimes et al., 2008; Van Tiem and Di Giulio, 2011). Each 25-μL QPCR reaction consisted of 12.5 μL SYBR Green PCR Master Mix (Applied Biosystems), 9.5 μL dH_2O, 200 nM each forward and reverse primer, and 4 ng cDNA template. The reactions were carried out using an Applied Biosystems 7300 Real-Time PCR System with a thermal profile of 10 min at 95 °C and 40 replicates of 15 s at 95 °C, 1 min at 60 °C. A dissociation curve was calculated for each sample at the end of each profile to confirm formation of a single product during the reaction. All samples were run in duplicate, and technical replicates were

averaged prior to analysis. The ABI PRISM 7300 Sequence Detection System Software, Version 1.1 (Applied Biosystems) was used to carry out data analysis. The average mRNA fold induction of each target gene was calculated by comparing the C_T (threshold cycle) of the target gene to that of β-actin according to Livak and Schmittgen (2001). β-Actin expression remained constant across treatments. Gene expression is expressed as fold-induction relative to DMSO controls.

2.7 Deformity assessment

At 96 hpf, hatched zebrafish embryos were screened for cardiac deformities via measurement of pericardial effusion. Embryos were removed from the dosing solution, rinsed with 30% Danieau, and anesthetized with MS-222. Fish were then placed on depression slides in the left lateral position in 3% methylcellulose and were imaged using light microscopy under 50x magnification (Zeiss Axioskop, Thornwood, NY, USA). The two-dimensional area of the pericardium was manually traced and then quantified using IPLab software (Scanalytics Inc., Fairfax, VA, USA). Deformity values are expressed as a percentage of the two-dimensional pericardial area of NI control embryos.

2.8 Statistical analysis

Statistical analyses were performed using JMP 8.1.1 (SAS Institute Inc., Cary, NC, USA). For *GSTp2* expression in NI embryos, the data were analyzed via one-way analysis of variance (ANOVA) followed by Tukey's post-hoc test. Deformity data were analyzed via two-way ANOVA to determine an overall effect of the morpholino injection and dose, followed by least square means (LSMeans) procedures. Tukey's post-hoc test was used to determine differences between groups. Experiments were replicated at least three times, and no differences between experimental replicates were observed. Data are represented as means ± standard error of the means (SEM). Values were considered significantly different at $p \leq 0.05$.

3. Results

3.1 GSTp2 mRNA expression in response to PAH and PCB-126 exposure

GSTp2 mRNA expression was induced by various PAH treatments and PCB-126 exposure. Exposure to 10 mg/L BkF induced *GSTp2* expression 2.3±0.3-fold over control levels ($p < 0.001$), and exposure to 10 mg/L BkF + 200 mg/L FL induced *GSTp2* expression greater than controls and BkF alone (5.7±0.8-fold, $p < 0.001$) (Fig. 1A). FL alone did not induce *GSTp2* expression above control levels. Exposure to 100 mg/L BaP and 100 mg/L BaP + 500 mg/L FL also induced *GSTp2* expression. BaP caused a 3.3±0.3-fold induction ($p = 0.012$), and BaP + FL caused a 7.0±0.9-fold induction above controls ($p < 0.01$); at this higher dose, FL did not significantly induce *GSTp2* expression above control levels (1.4±0.3-fold; Fig. 1B). At 1 mg/L, PCB-126 significantly induced *GSTp2* expression above control levels (2.9±0.7-fold, $p = 0.0229$; Fig. 1C).

3.2 Confirmation of morpholino efficacy by reverse transcription PCR analysis

Knockdown of GSTp2 was measured via RT-PCR and was demonstrated by comparing amplification of a cDNA fragment in the region targeted by the morpholino, exon 1 – 3, between NI and GSTp2-mo embryos. As shown in Fig. 2, neither NI nor GSTp2-mo embryos exposed to DMSO exhibited amplification of the GSTp2 cDNA fragment (lanes 2 and 3 and lanes 4 and 5, respectively). NI embryos exposed to BkF + FL exhibited strong amplification of the GSTp2 cDNA fragment (lanes 6 and 7). In contrast, GSTp2-mo embryos exposed to BkF + FL exhibited very weak amplification of the GSTp2 cDNA fragment and also exhibited weak amplification of a smaller band, indicating successful

knockdown of GSTp2 via deletion of the 36 base pair exon 2 by the splice-junction morpholino (lanes 8 and 9).

3.3 Deformity Assessment

The role of GSTp2 in ameliorating or exacerbating PAH-induced cardiotoxicity was examined via morpholino knockdown of the gene. NI, Co-mo, and GSTp2-mo embryos were exposed to various combinations of an AHR agonist (BkF or BaP) and a CYP1A inhibitor (FL). Embryos were also exposed to two concentrations of PCB-126. Two different GSTp2 morpholino concentrations, 100 mM and 250 mM, were used to determine if a greater concentration of morpholino would produce a greater effect. Injection of the Co-mo in DMSO control or dosed embryos did not cause any statistically significant differences in pericardial effusion as compared to NI DMSO control or dosed embryos ($p = 0.84$, data not shown). As we have shown in previous studies (Billiard et al., 2006; Van Tiem and Di Giulio, 2011), co-exposure to an AHR agonist and a CYP1A inhibitor caused cardiac deformities in embryonic zebrafish in this study. The severity of this cardiac toxicity was dependent upon the concentrations and types of PAHs used.

3.3.1 Influence of GSTp2 knockdown on deformities caused by BkF + FL co-exposure—Exposure to 100 mg/L BkF or 100 mg/L FL individually did not cause toxicity in NI embryos compared to controls; NI BkF-exposed embryos had an average pericardial area of 99±2% and NI FL-exposed embryos had an average pericardial area of 98±3% control pericardial area (Fig. 3A). Co-exposure to 100 mg/L BkF + 100 mg/L FL induced moderate but statistically significant pericardial effusion in NI embryos (120±3%; $p = 0.0001$). Neither concentration of GSTp2-mo caused toxicity in fish exposed to DMSO, BkF, or FL individually. Both the 100 and 250 mM GSTp2-mo exacerbated the pericardial effusion caused by 100 mg/L BkF + 100 mg/L FL exposure, resulting in average pericardial areas of 171±7% and 167±8%, respectively; these areas were significantly greater than the areas of NI fish of the same treatment (both $p < 0.0001$) but not different from one another.

GSTp2 knockdown also caused exacerbation of deformities caused by different concentrations of BkF and FL. In NI embryos and embryos injected with 100 mM and 250 mM GSTp2-mo, exposure to 10 mg/L BkF and 200 mg/L FL individually did not result in deformities (Fig. 3B). However, co-exposure to 10 mg/L BkF + 200 mg/L FL caused significant pericardial effusion in NI embryos (145±6%; $p < 0.0001$). This BkF +FL-induced effusion was exacerbated in fish injected with either 100 or 250 mM GSTp2-mo (213±12% and 205±12%, respectively; both $p < 0.0001$ vs. NI DMSO and NI BkF + FL and not different from one another).

3.3.2 Influence of GSTp2 knockdown on deformities caused by BaP + FL co-exposure—To test if deformity exacerbation by GSTp2 knockdown was unique to BkF + FL co-exposure, we also examined the effects of GSTp2 knockdown on the toxicity caused by co-exposure to FL and another AHR agonist, BaP. As with BkF and FL, exposure to 100 knockdown also caused exacerbation of deformities caused by different BaP or 500 knockdown also caused exacerbation of deformities caused by different FL alone did not cause pericardial effusion in NI or GSTp2-mo embryos (Fig. 3C). BaP + FL co-exposure caused moderate but significant pericardial effusion in NI embryos compared to NI controls (126±5%; $p < 0.001$). GSTp2 knockdown significantly exacerbated BaP + FL-induced pericardial effusion; 100 mM GSTp2-mo embryos had an average pericardial area of 147±6%, and 250 mM GSTp2-mo embryos had an average pericardial area of 145±6% (both $p < 0.001$ vs. NI DMSO and NI BkF + FL and not different from one another).

3.3.3 Influence of GSTp2 knockdown on deformities caused by PCB-126—In addition to PAH co-exposures, we also exposed NI and GSTp2-mo injected embryos to the strong AHR agonist, PCB-126. In NI embryos, 1 mg/L PCB-126 resulted in a slight but significant increase in pericardial effusion compared to controls (120±4%; $p = 0.02$; Fig. 4). In contrast to the interaction with PAH exposures, knockdown of GSTp2 with either concentration of morpholino did not exacerbate the deformities caused by 1 mg/L PCB-126 (124±5% in 100 mM GSTp2-mo embryos and 132±11% in 250 mM GSTp2-mo embryos; not significantly different from treated NI embryos or one another). NI embryos exposed to 2 mg/L PCB-126 had a pericardial area of 178±11% NI control area ($p < 0.001$ vs. NI DMSO). Once again, GSTp2 knockdown with either concentration of morpholino did not exacerbate the deformities caused by 2 mg/L PCB-126; 100 mM GSTp2-mo embryos had an average pericardial area of 172±9%, and 250 mM GSTp2-mo embryos had an average pericardial area of 179±14% (not significantly different from PCB-126-exposed NI embryos or one another).

4. Discussion

Our results show that knockdown of GSTp2 in zebrafish exacerbates the cardiac toxicity caused by co-exposures to a PAH that is an AHR agonist (BkF or BaP) and one that is a CYP1 inhibitor (FL), but does not affect the toxicity caused by the strong AHR agonist PCB-126.

The various GST isoforms have different specificities for different electrophilic metabolites of exogenous compounds. In particular, the mu and pi class GSTs show the highest activities with epoxides (Ketterer and Mulder, 1990). Because phase I metabolism of PAHs may result in the formation of epoxide metabolites, these two GSTs have received the most attention with regard to PAH metabolism and toxicity. GSTp activity was shown to be induced approximately two-fold over control levels in the livers of rainbow trout (*Oncorhynchus mykiss*) seven days after i.p. injection of BNF (Celander et al., 1993). In a similar study, hepatic GST activity was significantly increased 2.3-fold in adult rainbow trout 14 days after i.p. injection with 50 mg/kg body weight BNF (Zhang et al., 1990). In another study utilizing rainbow trout, *GSTp* expression was induced in juveniles exposed to crude oil or heavy fuel oil, a complex mixture of PAHs, for 96 h (Hook et al., 2010). *GST* mRNA expression was also shown to be induced after a 16-day exposure of juvenile thicklip grey mullet (*Chelon labrosus*) to weathered heavy fuel oil (Bilbao et al., 2010). It is likely that the induction of GSTs by AHR ligands occurs either by interaction of the AHR with a xenobiotic response element (XRE) or antioxidant response element (ARE) upstream of the GSTs. Both an XRE and ARE have been identified in the 5′ flanking region of rat GSTa (Rushmore et al., 1990; 1991), and rat GSTp and mouse GSTp1 also contain ARE-like sequences (Ikeda et al., 2004; Ikeda et al., 2002). Moreover, proximal and functional ARE-like sequences have been identified upstream of the transcription initiation sites in zebrafish GSTp1 and GSTp2 (Suzuki et al., 2005). It is currently unknown if zebrafish GSTp2 contains an XRE. However, we have previously shown that knockdown of the AHR2 in zebrafish results in decreased *GSTp2* expression in response to 50 mg/L BkF and 50 mg/L BkF + 150 mg/L FL exposure (Van Tiem and Di Giulio, 2011), suggesting that PAH induction of GSTp2 likely occurs through the AHR.

GSTp2 induction as well as the deformities caused by PAHs may also be a result of oxidative stress caused by PAHs. However, attempts to rescue PAH-induced deformities with the antioxidant n-acetyl cysteine or exacerbate deformities with buthionine sulfoxide, an inhibitor of the rate-limiting enzyme in GSH synthesis, glutamate-cysteine ligase, proved unsuccessful (Timme-Laragy et al., 2009). Thus, in response to PAHs, the role of GSTp2 in phase II metabolism may be of greater importance than its role in an oxidative stress

response. Identification of XREs or AREs in other zebrafish GST isoforms will help to elucidate the mechanism by which GSTs are induced by PAHs.

No other studies that we know of have knocked down GSTp in fish. However, *GstP1/P2*($^{-/-}$) mice exposed to a single topical application of the carcinogenic PAH 7,12-dimethylbenzanthracene and repeat applications of the tumor promoting agent 12-*O*-tetradodecanoyl-13-acetate had a 10-fold higher incidence of skin papillomas than *GstP1/P2*($^{+/+}$) mice (Henderson et al., 1998), indicating the protective function of GSTp isoforms in mice in response to the carcinogenic activity of PAHs. Even though the mechanisms by which PAHs induce carcinogenesis and developmental toxicity are most likely different, the pi class GSTs appear to serve a protective role in both of these processes. In another study examining a different GST isoform, *Gstz1*$^{-/-}$ mice had reduced liver glutathione levels and increased hepatotoxicity in response to acetaminophen via production of oxidative stress (Blackburn et al., 2006), showing the protective capacity of certain GSTs against drug-induced toxicity via AHR-independent mechanisms.

Because GSTs conjugate reactive epoxides and other electrophilic metabolites, the induction of GST expression and activity is often considered to be part of an adaptive response to toxicants (Hayes et al., 2005). Killifish from the Atlantic Wood Superfund site on the Elizabeth River in VA, a site contaminated with high levels of PAHs, were found to have GST levels six-fold higher than those of fish from a control site, whereas fish from an intermediate site had GST levels two-fold higher than those of reference site fish (Armknecht et al., 1998). Similarly, the GST activity in the liver of brown bullhead catfish (*Ameiurus nebulosus*) from a PCB-contaminated site was three-fold higher than in reference site fish (Otto and Moon, 1996). Our results also indicate that the presence and induction of GSTp2 is a protective response to PAH exposure. However, induction of GSTs does not necessarily equate to protection; PCB-126 induced *GSTp2* expression in our study, though to a much lesser extent than the PAH co-exposures, but knockdown of GSTp2 did not exacerbate PCB-126-induced deformities. The increased *GSTp2* expression may have been a result of reactive oxygen species (ROS) formed by PCB-126-induced uncoupling of the CYP1 catalytic cycle (Schlezinger et al., 2006). However, if ROS were produced, they were most likely scavenged by another antioxidant as GSTp2 does not appear to play a protective role in the cardiac toxicity caused by PCB-126 exposure.

As with PAHs, the inducibility of GSTs by PCBs seems to be species-, compound-, dose-, time-, assay-, and sex-dependent. For example, there was no change in GST activity in rainbow trout embryos after three or seven days of exposure to 1, 10, or 100 mg/L of another co-planar PCB, 3, 3′, 4, 4′-tetrachlorobiphenyl (PCB-77) (Koponen et al., 2000). PCB-126, at doses of 10 and 100 μg/kg body weight, was also incapable of inducing GST activity in adult male sea bass (*Dicentrarchus labrax*) (Vaccaro et al., 2005). However, PCBs have been shown to induce GST activity. In an early experiment in juvenile rainbow trout, BNF and Clophen A50, a commercial mixture of PCBs, both induced hepatic GST activity (Andersson et al., 1985). PCB-77 and PCB-126 also induced GST activity in rainbow trout six days after i.p. injection with 0.1 mg/kg or 0.5 mg/kg body weight (Huuskonen et al., 1996). Activity and expression data are not directly comparable, and QPCR is more sensitive than GST activity assays; however, we could not find examples of increased *GSTp2* expression in response to PCB-126 in the literature. While PAHs are rapidly metabolized via phase I and II metabolism, this is not the case for co-planar PCBs, such as PCB-126. Even though co-planar PCBs are capable of inducing CYPs and GSTs, they are not good substrates for the enzymes. A two-week PCB-126 exposure increased GST activity in rats but did not alter hepatic glutathione levels, perhaps indicating a lack of conjugation via GST (Lai et al., 2011). PCB-126 is much more slowly metabolized than the PAHs, and thus a comparatively smaller amount of PCB-126 metabolites are available for glutathione

conjugation via GSTs compared to PAH metabolites. For example, concentrations of PCB-126 in the liver of juvenile lake trout (*Salvelinus namaycush*) did not significantly change up to 30 weeks following PCB injection even though CYP1 activity remained greater than in controls (Palace et al., 1996). Coplanar PCBs such as PCB-126 are largely resistant to metabolism due to their high degree of chlorination (Safe, 1994). Thus, it is not unexpected that GSTp2 knockdown did not have an effect on the cardiac deformities caused by PCB-126 in this study.

In conclusion, *GSTp2* expression was induced by individual AHR agonists (BkF, BaP, and PCB-126) and even more highly by co-exposure to BkF + FL and BaP + FL in zebrafish embryos. Knockdown of GSTp2 exacerbated the cardiac toxicity caused by BkF + FL and BaP + FL but did not affect the toxicity induced by PCB-126 exposure. Though the molecular mechanisms by which a PAH that is an AHR agonist and one that is a CYP1 inhibitor induce synergistic cardiac toxicity are not yet fully elucidated, our results indicate that the pi class GSTs serve a protective function against this synergistic toxicity.

References

Andersson T, Pesonen M, Johansson C. Differntial induction of cytochrome P450-dependent monooxygenase, epoxide hydrolase, glutathione transferease and udp glucuronosyl transferase activities in the liver of rainbow trout by beta-naphthoflavone or Clophen A50. Biochem Pharmacol. 1985; 34:3309–3314. [PubMed: 3929791]

Armknecht SL, Kaattari SL, Van Veld PA. An elevated glutathione S-transferase in creosote-resistant mummichog (Fundulus heteroclitus). Aquat Toxicol. 1998; 41:1–16.

Bilbao E, Raingeard D, de Cerio OD, Ortiz-Zarragoitia M, Ruiz P, Izagirre U, Orbea A, Marigomez I, Cajaraville MP, Cancio I. Effects of exposure to Prestige-like heavy fuel oil and to perfluorooctane sulfonate on conventional biomarkers and target gene transcription in the thicklip grey mullet Chelon labrosus. Aquat Toxicol. 2010; 98:282–296. [PubMed: 20362344]

Billiard SM, Timme-Laragy AR, Wassenberg DM, Cockman C, Di Giulio RT. The role of the aryl hydrocarbon receptor pathway in mediating synergistic developmental toxicity of polycyclic aromatic hydrocarbons to zebrafish. Toxicol Sci. 2006; 92:526–536. [PubMed: 16687390]

Blackburn AC, Matthaei KI, Lim C, Taylor MC, Cappello JY, Hayes JD, Anders MW, Board PG. Deficiency of glutathione transferase zeta causes oxidative stress and activation of antioxidant response pathways. Mol Pharmacol. 2006; 69:650–657. [PubMed: 16278372]

Celander M, Leaver MJ, George SG, Forlin L. Induction of cytochrome P450 1A1 and conugating enzymes in rainbow trout (Oncorhynchus mykiss) liver - a time-course study Comp. Biochem Physiol C. 1993; 106:343–349.

Denison MS, Pandini A, Nagy SR, Baldwin EP, Bonati L. Ligand binding and activation of the Ah receptor. Chem-Biol Interact. 2002; 141:3–24. [PubMed: 12213382]

Donham RT, Morin D, Jewell WT, Lame MW, Segall HJ, Tjeerdema RS. Characterization of cytosolic glutathione S-transferases in juvenile Chinook salmon (Oncorhynchus tshawytscha). Aquat Toxicol. 2005; 73:221–229. [PubMed: 15935862]

Grimes AC, Erwin KN, Stadt HA, Hunter GL, Gefroh HA, Tsai HJ, Kirby ML. PCB126 Exposure disrupts zebrafish ventricular and branchial but not early neural crest development. Toxicol Sci. 2008; 106:193–205. [PubMed: 18660518]

Hayes JD, Flanagan JU, Jowsey IR. Glutathione transferases. Annu Rev Pharmacol Toxicol. 2005; 45:51–88. [PubMed: 15822171]

Henderson CJ, Smith AG, Ure J, Brown K, Bacon EJ, Wolf CR. Increased skin tumorigenesis in mice lacking pi class glutathione S-transferases. Proc Natl Acad Sci USA. 1998; 95:5275–5280. [PubMed: 9560266]

Hook SE, Lampi MA, Febbo EJ, Ward JA, Parkerton TF. Hepatic gene expression in rainbow trout (Oncorhynchus mykiss) exposed to different hydrocarbon mixtures Environ. Toxicol Chem. 2010; 29:2034–2043.

Hu X, Benson PJ, Srivastava SK, Xia H, Bleicher RJ, Zaren HA, Awasthi S, Awasthi YC, Singh SV. Induction of glutathione S-transferase π as a bioassay for the evaluation of potency of inhibitors of benzo(a)pyrene-induced cancer in a murine model. Int J Cancer. 1997; 73:897–902. [PubMed: 9399673]

Huuskonen S, LindstromSeppa P, Koponen K, Roy S. Effects of non-ortho-substituted polychlorinated biphenyls (Congeners 77 and 126) on cytochrome P4501A and conjugation activities in rainbow trout (Oncorhynchus mykiss). Comp Biochem Physiol C. 1996; 113:205–213.

Ikeda H, Nishi S, Sakai M. Transcription factor Nrf2/MafK regulates rat placental glutathione S-transferase gene during hepatocarcinogenesis. Biochem J. 2004; 380:515–521. [PubMed: 14960151]

Ikeda H, Serria MS, Kakizaki I, Hatayama I, Satoh K, Tsuchida S, Muramatsu M, Nishi S, Sakai M. Activation of mouse Pi-class glutathione S-transferase gene by Nrf2 (NF-E2-related factor 2) and androgen. Biochem J. 2002; 364:563–570. [PubMed: 12023900]

Incardona JP, Collier TK, Scholz NL. Defects in cardiac function precede morphological abnormalities in fish embryos exposed to polycyclic aromatic hydrocarbons. Toxicol Appl Pharmacol. 2004; 196:191–205. [PubMed: 15081266]

Ketterer, B.; Mulder, G. Glutathione conjugation. In: GJ, M., editor. Conjugation Reactions in Drug Metabolism. Taylor and Francis; London: 1990. p. 307-364.

Kim JH, Dahms HU, Rhee JS, Lee YM, Lee J, Han KN, Lee JS. Expression profiles of seven glutathione S-transferase (GST) genes in cadmium-exposed river pufferfish (Takifugu obscurus). Comp> Biochem Physiol C. 2010; 151:99–106.

Koponen K, Lindstrom-Seppa P, Kukkonen JVK. Accumulation pattern and biotransformation enzyme induction in rainbow trout embryos exposed to sublethal aqueous concentrations of 3,3′,4,4 ′-tetrachlorobiphenyl. Chemosphere. 2000; 40:245–253. [PubMed: 10665414]

Lai IK, Chai Y, Simmons D, Watson WH, Tan R, Haschek WM, Wang K, Wang B, Ludewig G, Robertson LW. Dietary selenium as a modulator of PCB 126–induced hepatotoxicity in male Sprague-Dawley rats. Toxicol Sci. 2011; 124:202–214. [PubMed: 21865291]

Leaver MJ, Wright J, George SG. Structure and expression of a cluster of glutathione S-transferase genes from a marine fish, the plaice (Pleuronectes platessa). Biochem J. 1997; 321:405–412. [PubMed: 9020873]

Livak KJ, Schmittgen TD. Analysis of relative gene expression data using real-time quantitative PCR and the 2(T)(-Delta Delta C) method. Methods. 2001; 25:402–408. [PubMed: 11846609]

Nasevicius A, Ekker SC. Effective targeted gene ‘knockdown’ in zebrafish. Nat Genet. 2000; 26:216–220. [PubMed: 11017081]

Nebert DW, Roe AL, Dieter MZ, Solis WA, Yang Y, Dalton TP. Role of the aromatic hydrocarbon receptor and [Ah] gene battery in the oxidative stress response, cell cycle control, and apoptosis. Biochem Pharmacol. 2000; 59:65–85. [PubMed: 10605936]

Otto DME, Moon TW. Phase I and II enzymes and antioxidant responses in different tissues of brown bullheads from relatively polluted and non-polluted systems. Arch Environ Contam Toxicol. 1996; 31:141–147. [PubMed: 8688001]

Palace VP, Klaverkamp JF, Lockhart WL, Metner DA, Muir DCG, Brown SB. Mixed-function oxidase enzyme activity and oxidative stress in lake trout (Salvelinus namaycush) exposed to 3,3′, 4,4′,5-pentachlorobiphenyl (PCB-126). Environ Toxicol Chem. 1996; 15:955–960.

Robertson IGC, Guthenberg C, Mannervik B, Jernström B. Differences in stereoselectivity and catalytic efficiency of three human glutathione transferases in the conjugation of glutathione with 7β,8α-dihydroxy-9α,10α-oxy-7,8,9,10-tetrahydrobenzo(a)pyrene. Cancer Res. 1986; 46:2220–2224. [PubMed: 3084065]

Rushmore TH, King RG, Paulson KE, Pickett CB. Regulation of glutathione s-transferase ya subunit gene expression - indentification of a unique xenobiotic-responsive element controlling inducible expression by planar aromatic compounds Proc. Natl Acad Sci USA. 1990; 87:3826–3830.

Rushmore TH, Morton MR, Pickett CB. The antioxidant responsive element - activation by oxidative stress and identification of the DNA consensus sequence required for functional activity. J Biol Chem. 1991; 266:11632–11639. [PubMed: 1646813]

Safe SH. Polychlorinated Biphenyls (PCBs): Environmental Impact, Biochemical and Toxic Responses, and Implications for Risk Assessment. Crit Revs Toxicol. 1994; 24:87–149. [PubMed: 8037844]

Schlenk, D.; Celander, M.; Gallagher, EP.; George, S.; James, M.; Kullman, SW.; van den Hurk, P.; Willett, K. Biotransformation in fishes. In: DiGiulio, RT.; Hinton, DE., editors. Toxicology of Fishes. Crc Press-Taylor & Francis Group; Boca Raton: 2008. p. 153-234.

Schlezinger JJ, Struntz WDJ, Goldstone JV, Stegeman JJ. Uncoupling of cytochrome P450 1A and stimulation of reactive oxygen species production by co-planar polychlorinated biphenyl congeners. Aquat Toxicol. 2006; 77:422–432. [PubMed: 16500718]

Schmidt JV, Bradfield CA. Ah receptor signaling pathways. Annu Rev Cell Dev Biol. 1996; 12:55–89. [PubMed: 8970722]

Suzuki T, Takagi Y, Osanai H, Li L, Takeuchi M, Katoh Y, Kobayashi M, Yamamoto M. Pi class glutathione S-transferase genes are regulated by Nrf2 through an evolutionarily conserved regulatory element in zebrafish. Biochem J. 2005; 388:65–73. [PubMed: 15654768]

Tillitt, DE.; Cook, PM.; Giesy, JP.; Heideman, W.; Peterson, RE. Reproductive impairment of Great Lakes lake trout by dioxin-like chemicals. Crc Press-Taylor & Francis Group; 2008.

Timme-Laragy AR, Van Tiem LA, Linney EA, Di Giulio RT. Antioxidant Responses and NRF2 in Synergistic Developmental Toxicity of PAHs in Zebrafish. Toxicol Sci. 2009; 109:217–227. [PubMed: 19233942]

Vaccaro E, Meucci V, Intorre L, Soldani G, Di Bello D, Longo V, Gervasi PG, Pretti C. Effects of 17[beta]-estradiol, 4-nonylphenol and PCB 126 on the estrogenic activity and phase 1 and 2 biotransformation enzymes in male sea bass (Dicentrarchus labrax). Aquat Toxicol. 2005; 75:293–305. [PubMed: 16219370]

Van Tiem LA, Di Giulio RT. AHR2 knockdown prevents PAH-mediated cardiac toxicity and XRE- and ARE-associated gene induction in zebrafish (Danio rerio). Toxicol Appl Pharmacol. 2011; 254:280–287. [PubMed: 21600235]

Wassenberg DM, Di Giulio RT. Synergistic embryotoxicity of polycyclic aromatic hydrocarbon aryl hydrocarbon receptor Agonists with cytochrome P4501A inhibitors in Fundulus heteroclitus. Environ Health Perspect. 2004; 112:1658–1664. [PubMed: 15579409]

Zhang YS, Andersson T, Förlin L. Induction of hepatic xenobiotic biotransformation enzymes in rainbow trout by [beta]-naphthoflavone. Time-course studies. Comp Biochem Physiol B. 1990; 95:247–253.

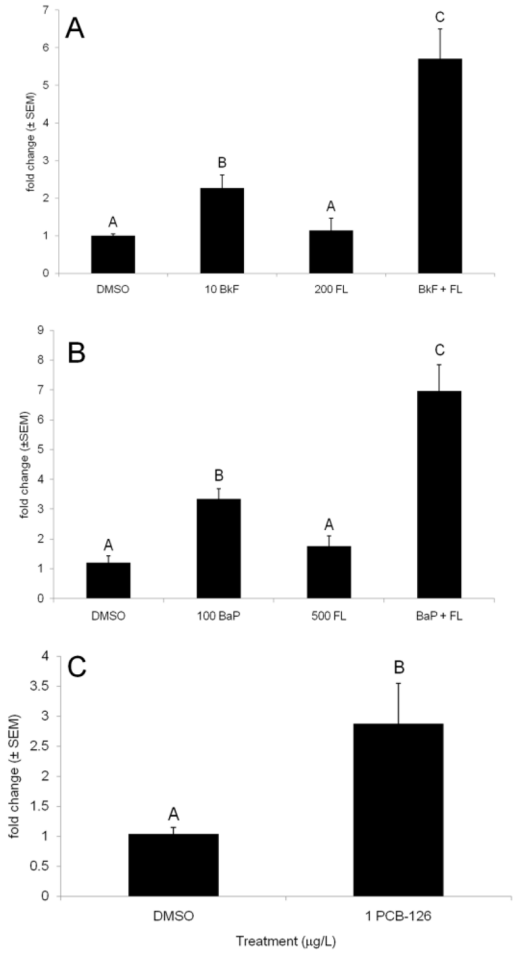

Fig. 1.

Effect of PAHs and PCB-126 on *GSTp2* gene expression. A) 10 mg/L BkF and 200 mg/L FL; B) 100 mg/L BaP and 500 mg/L FL; and C) 1 mg/L PCB-126. Expression is shown as fold induction compared to DMSO controls. n = 9 per treatment; each n represents 10 pooled embryos. Groups not sharing a common letter are significantly different ($p \leq 0.05$; ANOVA, Tukey's post-hoc test).

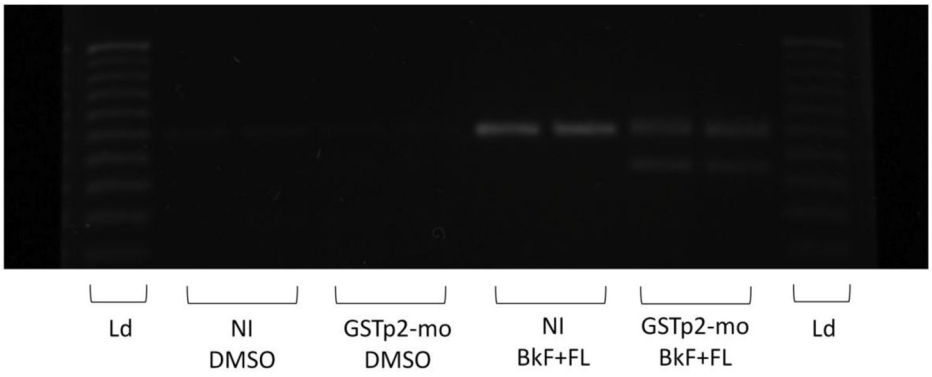

Fig. 2.

Effective knockdown of GSTp2 via splice junction morpholino in embryos exposed to DMSO or 10 mg/L BkF + 200 mg/L FL at 24 hpf. Representative image is from RT-PCR amplification of 10 pooled embryos per each treatment. Ld = 25 bp DNA ladder (lanes 1 and 10). NI embryos exposed to BkF + FL show strong amplification of the GSTp2 exon 1 –3 cDNA fragment (lanes 6 and 7). BkF + FL-exposed GSTp2-mo embryos exhibit weaker amplification of the GSTp2 exon 1–3 cDNA fragment and exhibit weak amplification of a smaller band, indicating deletion of exon 2 by the GSTp2-mo (8 and 9).

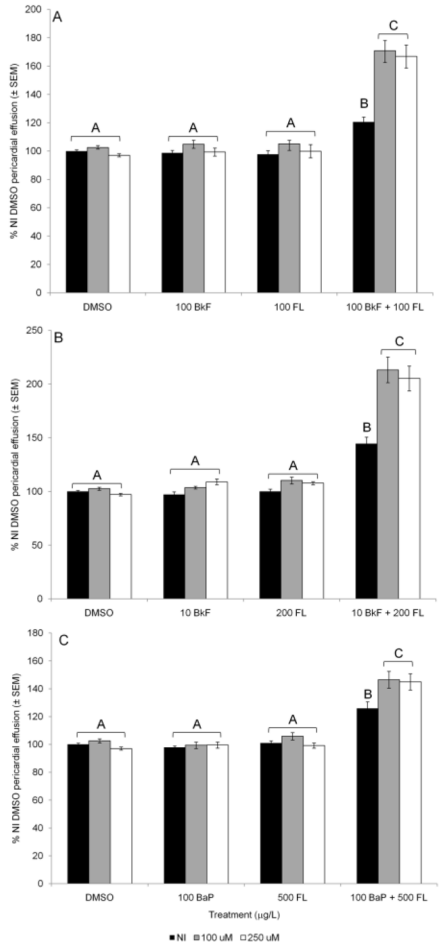

Fig. 3.

PAH-induced deformities in NI and GSTp2-mo injected embryos. A) 100 mg/L BkF and 100 mg/L FL; B) 10 mg/L BkF and 200 mg/L FL; C) 100 mg/L BaP and 500 mg/L FL. Embryos were dosed at 24 hpf and scored at 96 hpf. NI embryos are represented by black bars, 100 mM GSTp2-mo embryos are represented by grey bars, and 250 mM GSTp2-mo embryos are represented by white bars. Deformities are expressed as percent NI control (DMSO) pericardial effusion ± SEM (n = 12 per treatment; each n represents the average of five embryos). Groups not sharing a common letter are significantly different ($p \leq 0.05$; ANOVA, Tukey adjusted LSMeans).

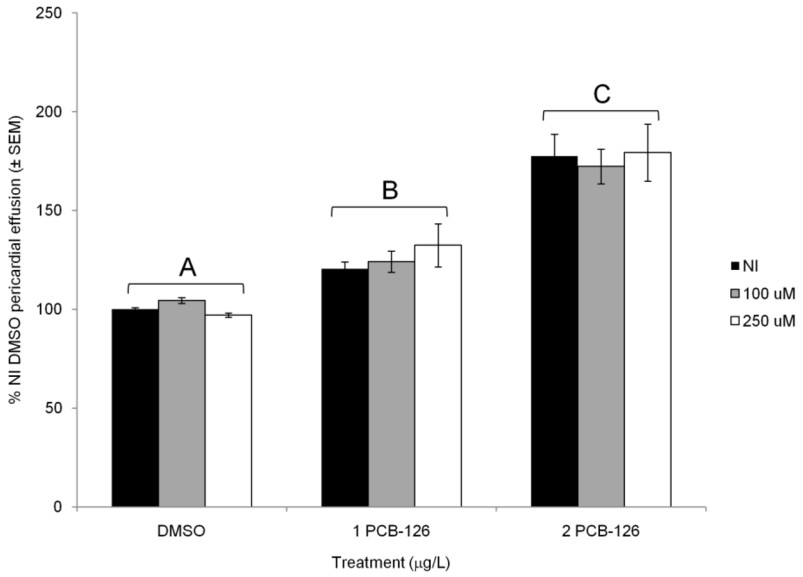

Fig. 4.

PCB-126-induced deformities in NI and GSTp2-mo injected embryos. Embryos were dosed with DMSO, 1 mg/L PCB-126, or 2 mg/L PCB-126 at 24 hpf and scored at 96 hpf. NI embryos are represented by black bars, 100 mM GSTp2-mo embryos are represented by grey bars, and 250 mM GSTp2-mo embryos are represented by white bars. Deformities are expressed as percent NI control (DMSO) pericardial effusion ± SEM (n = 12 per treatment; each n represents the average of five embryos). Groups not sharing a common letter are significantly different ($p \leq 0.05$; ANOVA, Tukey adjusted LSMeans).